



DOI: 10.5281/zenodo.1256057

TECHNOLOGY AND BUILDING MATERIALS IN ROMAN AGE (1st BC - 2nd AD): THE "MAUSOLEO DELLA SFINGE" FROM THE ARCHAEOLOGICAL SITE OF CUMA (ITALY)

Sossio Fabio Graziano^{1*}, Claudia Di Benedetto¹, Vincenza Guarino¹, Concetta Rispoli¹, Priscilla Munzi², Piergiulio Cappelletti¹, Vincenzo Morra¹

¹Dipartimento di Scienze della Terra, dell'Ambiente e delle Risorse, Università degli Studi di Napoli, Federico II, Via Cintia 26, 80126 Napoli, Italia

²Centre Jean Bérard (USR 3133 CNRS-EFR), Napoli, Italia

Received: 17/11/2017

Accepted: 29/01/2018

*Corresponding author: Sossio Fabio Graziano (sgraziano@unina.it)

ABSTRACT

This research aims to deepen knowledge on geomaterials used in building operations of a very important monumental complex belonging to the "Porta Mediana" necropolis the archeological site of Cuma.

The entire site counts 70 mausoleums among which, the one named "Sphinx complex" or A63, is particularly important. For its realization several geomaterials have been used.

Analytical results were carried out from several techniques such as optical microscopy, microchemical and mineralogical-petrographical analysis, scanning electron microscopy with EDS and X-ray powder diffraction. This approach allows to clarify the provenance of natural geomaterials and also the technological processes involved in the production of artificial geomaterials (mortars, plasters, *cocciopesto*).

Phlegrean tuffs, due to their easy workability and good mechanical features, were used mainly for masonries and for decorative function (a bas-relief of a "sphinx" for example). As far as artificial geomaterials are concerned, the use of a volcanic aggregate, was privileged too. Some examples of imported stones were also found: limestones and marbles, the first one implemented as a building material for *cippi* of the fence while the second one for prestigious coating elements. Results permitted to evaluate building techniques of the period and mainly the wide potential of Phlegrean fields' materials when used as a bulding stone. This research aims also to give important informations for restoring and conservative actions useful for mausoleums of the entire site.

KEYWORDS: Cuma, necropolis, Roman age, sphinx complex, archaeometry, geomaterials, analytical techniques

1. INTRODUCTION

Archaeometric studies on geomaterials from archaeological sites are commonly very useful to identify raw materials used in the building operations and to obtain information on provenance (e.g. Mahmoud *et al.*, 2012). This kind of researches is also able to determine the technological processes involved in the production of artificial geomaterials (mortars, plasters, *cocciopesto*), revealing important information on the history of buildings and their different construction phases.

The study area is located in Campania region (southern Italy), that, from the geological point of view, is largely dominated by Phlegraean Fields and Somma-Vesuvius volcanic district, accompanied by the Sorrento peninsula (along with Capri island) with its sedimentary carbonatic series. This geological context provides geomaterials with high availability and good petrophysical features used, since ancient times, in local architecture (de Gennaro *et al.*, 2013 and references therein). The archaeological site of Cuma is an outstanding example of this utilization. Part of the archaeological area is represented by the funeral site named "Porta Mediana" necropolis (Fig. 1), known since the seventeenth century, and revealed by the Centre Jean Bérard archaeologists between 2001 and present, counting something like 70 tombs belonging from 4th BC to 6th century AD time range. Among funerary buildings, the "Complesso monumentale della Sfinge" (identified by the ID: A63), so named for the presence of a sphinx sculpture (Fig. 2a) found on the monumental facade, dated back to the end of 1st century BC and was used as burial place until the 2nd century AD (Brun *et al.*, 2017). A63 complex is important and interest-

ing not only for archaeological reasons, such as the chronological building period, the mausoleum location, the particulars (fence and mausoleum), the types of burials (cremation and inhumation), but also for the geological point of view. This funerary complex is unique in its kind, as it shows use of the widest variety of geomaterials both for the masonry and for decorative apparatus (yellow tuff, grey tuff, mortar, *cocciopesto*, limestone, marble).

The goal of this research is to study geomaterials used in A63 complex in order to, through mineralogical and petrographic approach: a) characterise building materials; b) provide some hypotheses on their provenance. This approach can be considered as a mandatory basis to allow right actions both for the conservation and a conscious fruition of cultural heritage.

2. MONUMENT DESCRIPTION

The A63 funerary monument, investigated during two excavation campaigns in 2006 and 2009, is made up of a fence enclosing a monumental tomb and is located at 110 m W of *Porta Mediana*, along the road axis that bordered western walls of the necropolis.

The monumental balustrade front is made of large carved grey tuff blocks, while perimetral walls are realized with *opus reticulatum* technique with yellow tuff blocks. Large grey tuff slabs were used also for the floor of part of the fence to create a terraced basement. On the outer side of the perimeter, there is a tank, built in *opus reticulatum* with yellow tuff blocks and covered by a thick layer of *cocciopesto*. The tank was connected to a fountain on the facade (Fig. 1).

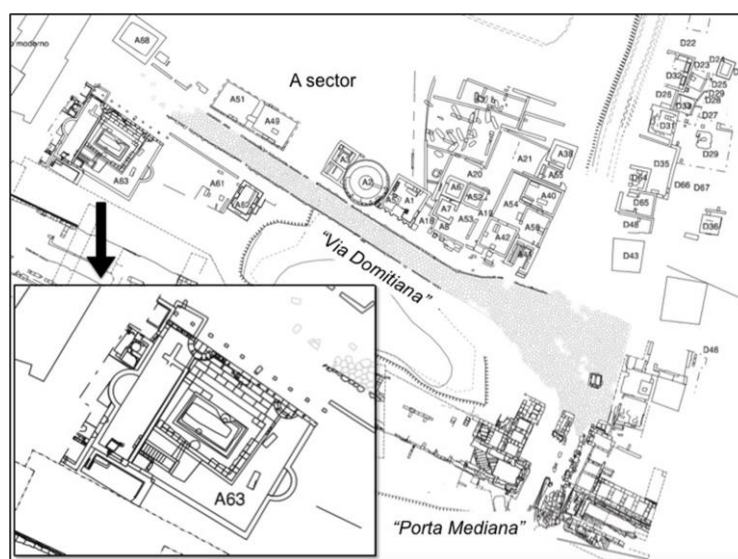


Figure 1. Schematic map of the archaeological area of Porta Mediana Necropolis (Cuma-Italy). In the box a focus on A63 mausoleum.

The actual mausoleum was lined with limestone blocks, still partially preserved in the SW corner, and decorated in bas-relief, as evidenced by a fragment of white corner marble block with a frieze (Fig. 2a).

The tall structure covered a hypogeal funerary room, accessible by a staircase located at the mausoleum SW corner. The internal organization of the funeral chamber presents some peculiar aspects. The E and W sides of the room are occupied by two brick beds to accommodate the burials. The N side was arranged to accommodate two tanks in which the remains of two cremated individuals were deposited.

The archaeological study of the monument recognized at least four building phases. The first corre-

sponds to the construction of fence, tank, the monumental facade and the basement and dates back to the *Augusteo-Tiberian* age. In this phase the burial space is defined by a wall made up with *opus reticulatum* technique with yellow tuff blocks. During the 1st century AD, in the second phase, only small constructive interventions (like a step addition to access ladder) were carried out. A third phase, corresponding to the *via Domitiana* construction time, contemplated the partial obliteration of the burial complex, while in the fourth construction phase, the N/S wall was built in *opera reticulata* always with yellow tuff blocks. The complex was completely abandoned in the last decades of the 3rd century AD.

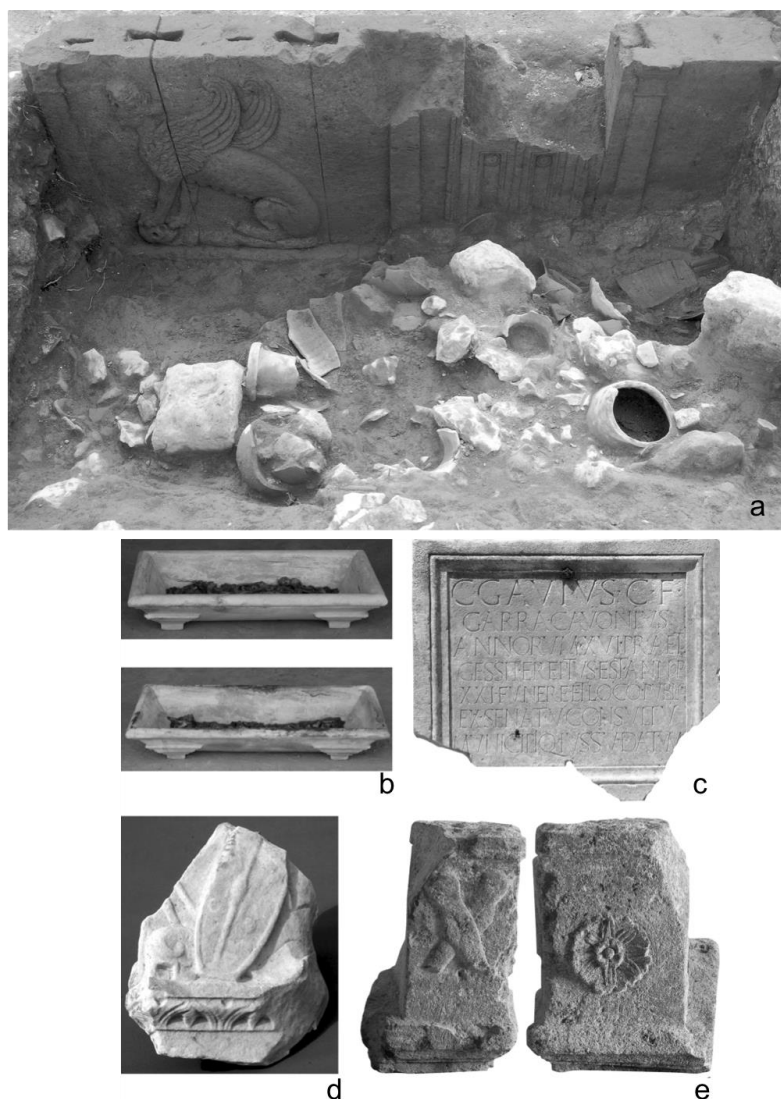


Figure 2. Archaeological finds from A63 mausoleum's excavation campaigns (modified after Brun et al., 2017). The study of the monument and the epigraph analysis allows to identify Caius Gavius Garra Cavonius and his family as the owners of the funerary building (A63).

In 2009, during the expansion of excavation on the W side of the complex, an epigraph was found. The

inscription summarizes, in few lines, the story of an illustrious character named *Caius Gavius Garra Ca-*

vonius, a 16 years old praetor. As reported by the inscription (Fig. 2b), the young man was part of an important family in *Giulio-Claudia* age and died when he was 21, before his *cursus honorum* was over. The honor of his social position was renewed, with his death, giving him public funerals and a public burial place very close to one of the main gates of the city (Brun *et al.*, 2017).

3. GEOLOGICAL SETTINGS

The archaeological area of *Porta Mediana* necropolis (Cuma) is located in the northwestern side of the Phlegraean Fields volcanic area (Melluso *et al.*, 2012) (Fig. 3). Phlegraean Fields represent a volcanic field set in the northern sector of the Bay of Naples. Its activity, mainly explosive, extends even in marine environments with the Ischia and Procida islands (De Astiis *et al.*, 2004).

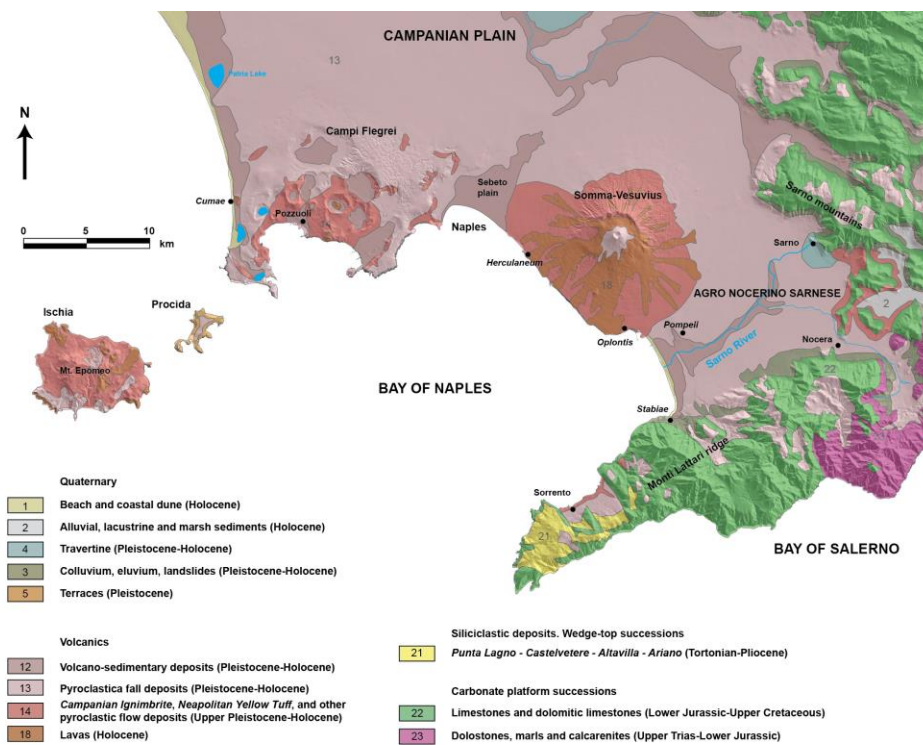


Figure 3. Geological map of Phlegraean Fields area (modified after De Bonis *et al.*, 2016).

The geological history of the area has been dominated by two main volcanic events: Campanian Ignimbrite ($^{40}\text{Ar}/^{39}\text{Ar}$, 39 ky; Fedele *et al.*, 2008) and Neapolitan Yellow Tuff ($^{40}\text{Ar}/^{39}\text{Ar}$ 15 ky; Deino *et al.*, 2004) eruptions. These events are related to two collapse episodes that, overlapping, generated a complex caldera representing the most evident structure of the Phlegraean volcanic district (Orsi *et al.*, 1996; Perrotta *et al.*, 2006). Phlegraean products belong to the alkaline-potassic series with shoshonitic affinity (Conticelli *et al.*, 2004). The most widespread lithotypes are the trachytes with the following most abundant minerals: clinopyroxene, plagioclase, alkali feldspar (sanidine), biotite and magnetite. Both events generated huge deposits of geomaterials commonly used in building sector since ancient times.

4. MATERIALS AND METHODS

Sampling was carried out under close supervision of archaeologists in order to preserve integrity of the monument and to get representative materials to investigate.

Studied geomaterials are the following:

- Tuffs: yellow tuffs samples respectively from the external wall (*opera reticulata* blocks - A63YT) and from the tank (*opera reticulata* blocks - A63YTT); grey tuff sample from the ornaments (A63GT).
- Mortars: binder between blocks from *opera reticulata* (A63M).
- *Cocciopesto*: two different samples belonging respectively to main building (A63C) and to tank (A63C2).
- Limestones: one sample from one in ten *cippi* (border signs consisting of a column or pillar

trunk) delimiting the mausoleum from the Via Domitiana (A63L).

- Marbles: one sample from a lining block with a frieze (A63MA)

Sampling points are reported in Fig. 4.

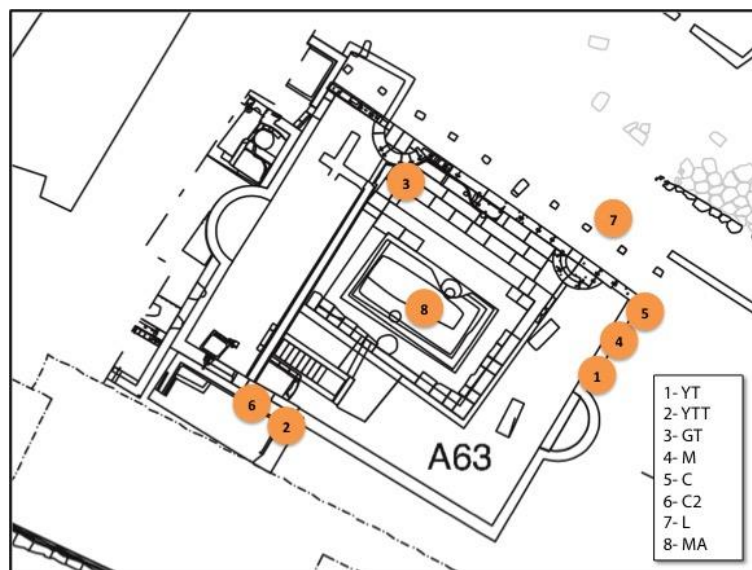


Figure 4. Sampling map. Legend of samples: YT = yellow tuff, wall; YTT = Yellow Tuff, tank; GT = Grey Tuff, ornament; M = Mortar, C and C2 = cocciopesto, L = Limestone, MA = Marble.

Experimental investigations include optical microscopy (OM), microchemical and mineralogical-petrographical analysis (SEM-EDS). Optical microscopy allowed to obtain information on texture and main components of samples. Image acquisition and grain size measurements were carried out using a Leitz Laborlux 12 POL microscope equipped with a Leica DFC280 camera and Leica Q Win image analysis software and following the terminology reported in UNI11305:2009 standard recommendations.

Microchemical analysis of minerals, glass phases and ceramic fragments were determined, through spot analyses, with a scanning electron microscope coupled with an Energy Dispersive Spectrometer (SEM-EDS) Oxford Instruments Microanalysis Unit and a JEOL JSM-5310 microscope operating at a 15 kV primary beam voltage, 50-100 mA filament current, a 15-17 μm spot size and a net acquisition time of 50 s. Measurements were done with an INCAX-stream pulse processor. Details of standards are provided in Melluso et al. (2017) and Guarino et al. (2017).

Mineralogical analyses were carried out by X-ray diffraction (XRPD) with Panalytical X'Pert Pro diffractometer equipped with a RTMS X'Cellerator de-

tector with the following operative conditions: CuK α radiation, 40 kV, 40 mA, 2 θ range from 4° to 70°, equivalent step size 0.017° 2 θ , 60 s per step counting time. Samples for XRPD analysis were prepared using a McCrone micronising mill (wet grinding time 15 min with agate cylinders to obtain <10 μm final grain size) or dry crushing by hand in agate mortar, in order to prevent (for binders) any loss of information on soluble phases. The software for identification of mineral phases was Panalytical Highscore Plus 3.0e with PDF2 and ICSD databases.

5. RESULTS

Macroscopic and microscopic observations

Yellow tuffs samples show very similar characteristics. Macroscopically, a prevailing yellow cineritic matrix with components variable in size (up to 7 mm for A63YT and 9 mm for A63YTT) can be observed. Thin section observations show, for both samples, a vitrophyric structure consisting in a brown ash matrix with abundant glassy shards, quite devitrified, in which pumice, obsidian, and loose crystals of alkali feldspar (sanidine), clinopyroxene and rare plagioclase are reported (Fig. 5).

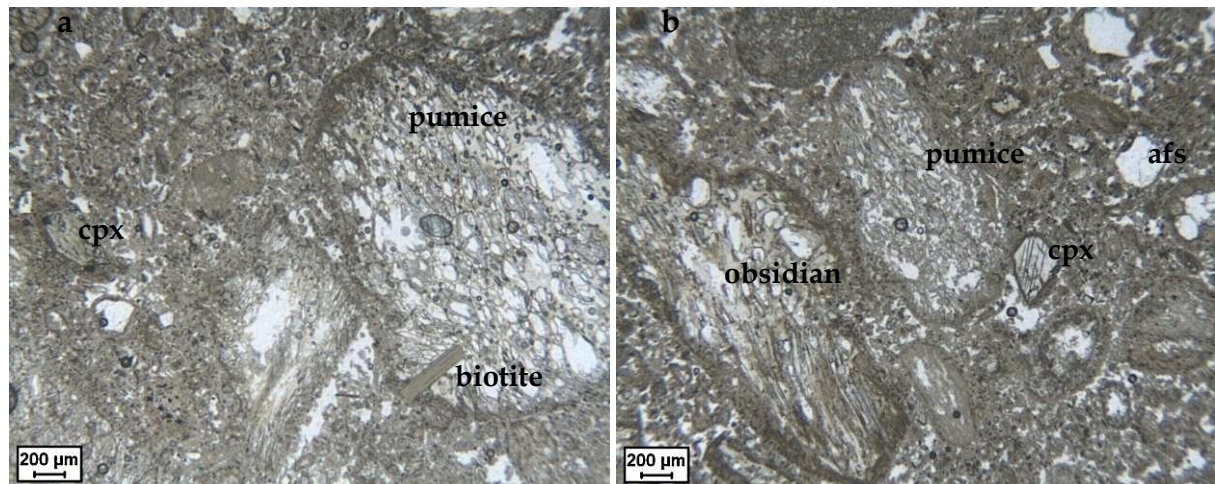


Figure 5. Micrographs (parallel polars) of A63YT (a) and A63YTT (b) samples.
Abbreviations: *cpx*, clinopyroxene; *afs*, alkali feldspar.

Grey tuff sample (A63GT), shows a dominant grey cineritic matrix, with feldspars and mica (biotite). Thin section observations (Fig. 6) show a vitrophyric texture, consisting of a grey ash matrix with

abundant glassy shards, in which pumice, loose crystals of alkali feldspar (sanidine), clinopyroxene, plagioclase, rare volcanic fragments, *fiamma*, and biotite are present.

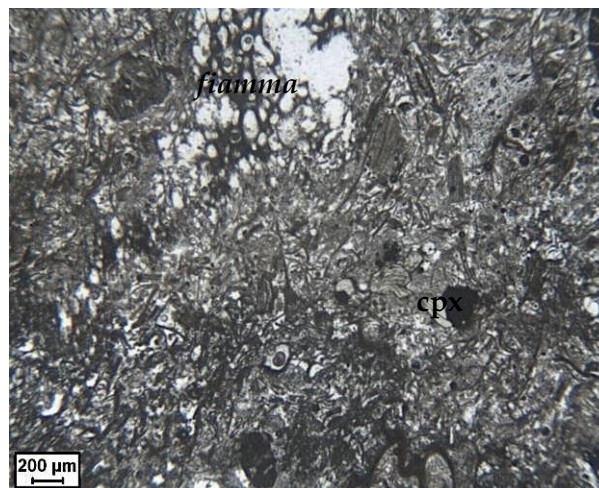


Figure 6. Micrograph (parallel polars) of A63GT sample.
Abbreviation: *cpx*, clinopyroxene.

The analyzed mortar (A563M) is constituted by a light brown matrix with abundant presence of aggregates. OM reveals that the matrix appears homogeneous and thickened (Fig. 7), aggregates (up to 5 mm in size) not oriented. Matrix has carbonatic composition and medium porosity due to shrinkage cracks. Aggregates are, in order of abundance, pumice and obsidian, crystal fragments of alkali feldspar, plagioclase, clinopyroxene, and mica (Fig. 7). Sporadic presence of white lumps is observable. A good adhesion between aggregates and binder is detectable.

Two *cocciopesto* samples (Fig. 8a-c) are both constituted by brown carbonatic matrix with clasts, variable in size from few microns up to 9 mm in A63C2 and 11 mm in A63C respectively. The carbonatic matrix is homogeneous with pottery fragments, pumices, obsidian, and loose crystals of alkali feldspar, plagioclase, clinopyroxene, and secondary mica. Sometimes white lumps are present. Both samples show medium porosity due to shrinkage cracks. A good adhesion between aggregates and binder matrix, due to recrystallization processes of calcite is also recognized.

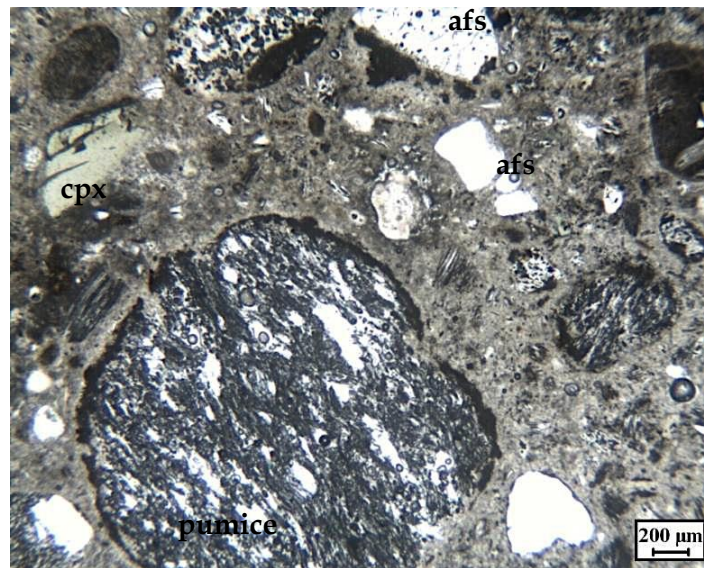


Figure 7. Micrograph (parallel polars) of A63M sample. Abbreviations: cpx, clinopyroxene; afs, alkali feldspar.

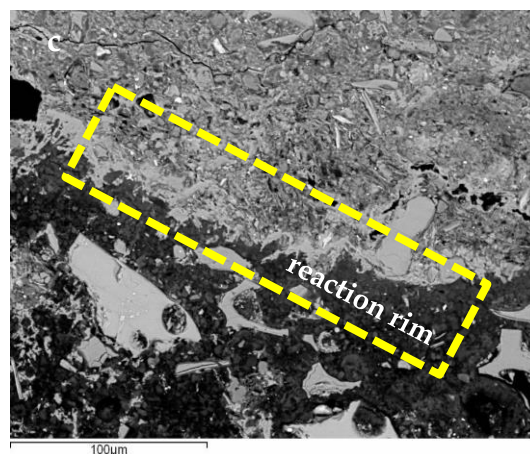
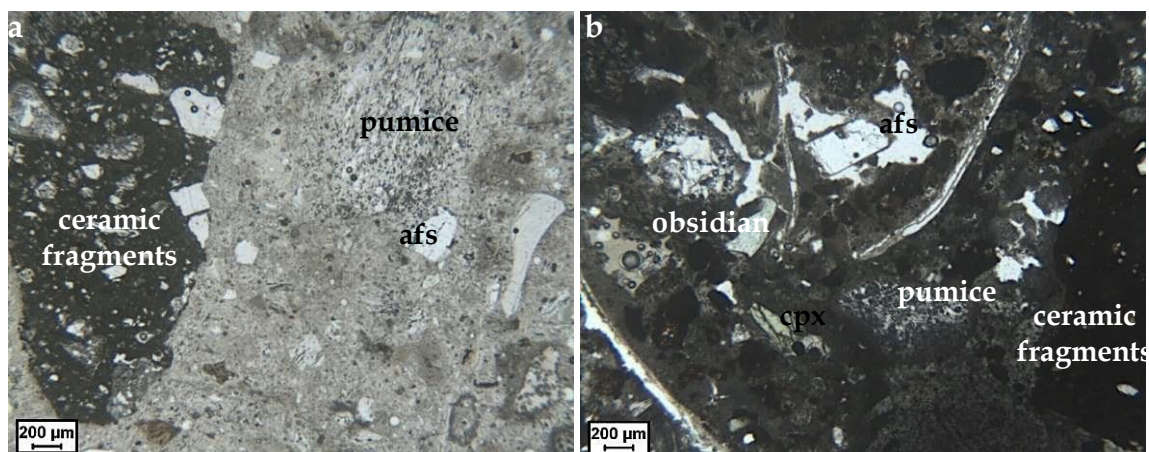


Figure 8. Polarized light images (parallel polars) of A63C (a) and A63C2 (b) samples. Evidence of hydraulicity (reaction rim) observed by SEM, in A63C sample (c). Abbreviations: cpx, clinopyroxene; afs, alkali feldspar.

The results of SEM observations allowed to consider a high hydraulicity of mortars associated to the abundant presence of materials with “pozzolanic” activity (ceramic and volcanic fragments) because the reactive silica contained in the aggregates reacts with calcium hydroxide, leading to the formation of calcium silicate hydrates: the so-called C-A-S-H phases (calcium, aluminum; silicate, hydrate). This

reaction is evident by the presence of reaction rims rounding ceramic fragments (Fig. 8c, De Luca *et al.*, 2015).

The A63L sample, a micritic limestone, shows a grey-white matrix, with medium to fine texture. It is made exclusively of calcite crystals (Fig. 9a,b). Evident cracks with from fine to microcrystalline carbonates are reported.

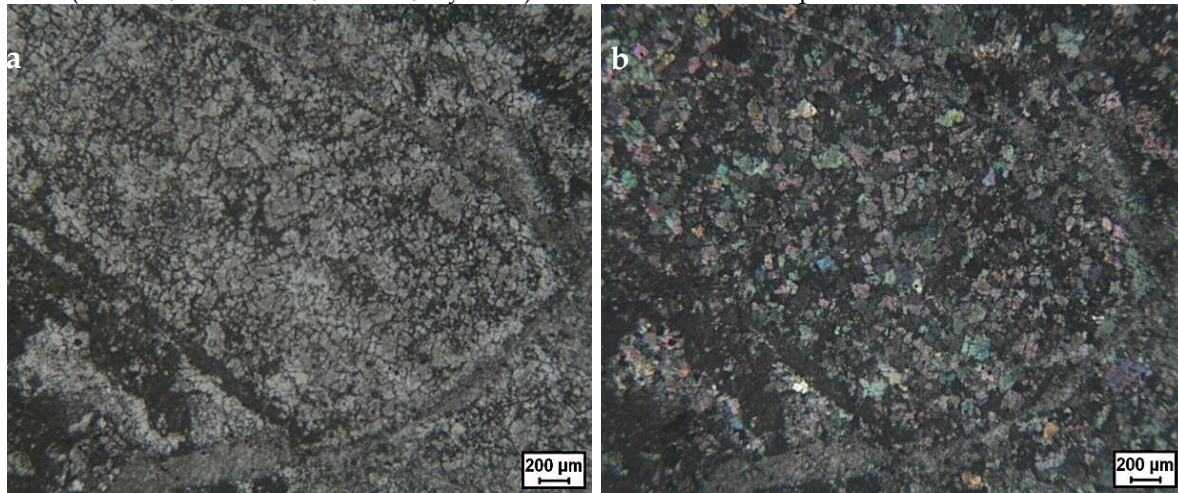


Figure 9. Polarized light images, parallel (a) and crossed (b) polars of A63L sample.

The marble sample (A63MA), white in colour, show a very homogeneous texture exclusively made

of carbonate grains (principally calcite) with medium-large dimension of crystals (Fig. 10 a,b).

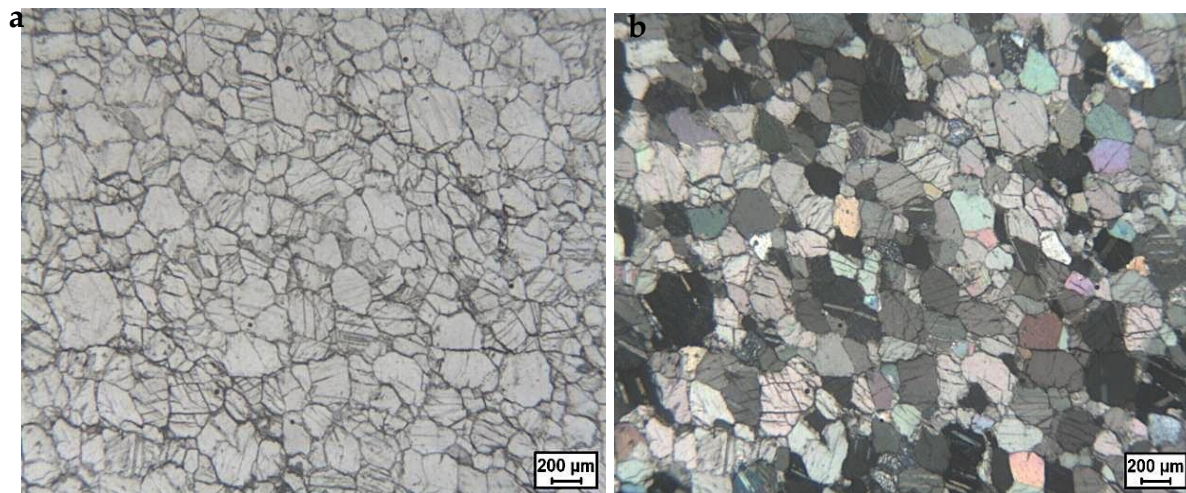


Figure 10. Polarized light images, parallel (a) and crossed (b) polars of A63MA sample.

Phase chemistry (EDS analysis)

This analysis was performed on juvenile materials, mainly glasses as pumice and/or obsidian, identified by OM. Results are listed in Table 1 and classified according to TAS diagram (Fig. 12).

The analysed glasses from samples A63YT and A63YTT, show a quite similar chemical composition, SiO_2 vary between 56.2 and 58.4 wt.% and $\text{Na}_2\text{O}+\text{K}_2\text{O}$ between 11 and 12.7 wt.%. Two zeolites, phillipsite and chabazite, were analyzed on the rim of altered glasses (Table 2 and Fig. 11).

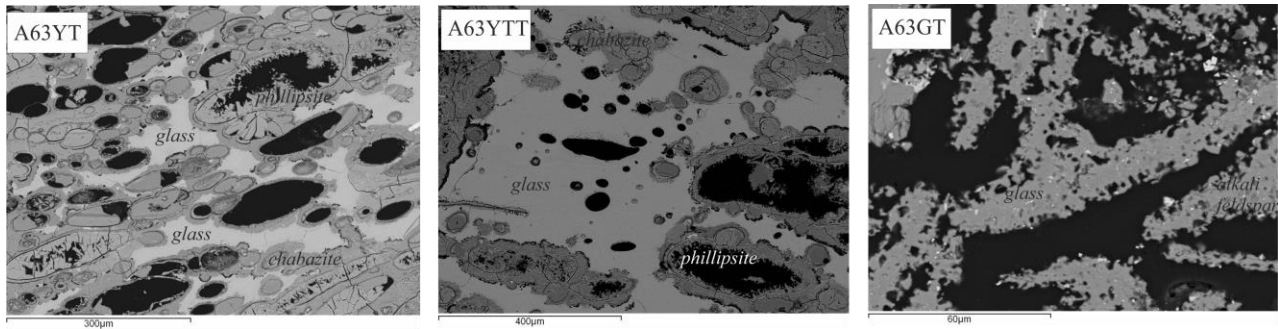


Figure 11. Representative backscattering images of tuffs samples.

Table 1. Glasses (pumice and obsidian) analyses from tuffs, mortars and cocchiopesto samples.

Tuffs	A63YT <i>glass</i>	A63YT <i>glass</i>	A63YT <i>glass</i>	A63YT <i>glass</i>	A63YT <i>glass</i>	A63YTT <i>glass</i>	A63YTT <i>glass</i>	A63YTT <i>glass</i>	A63YTT <i>glass</i>	A63GT <i>glass</i>	A63GT <i>glass</i>	A63GT <i>glass</i>
SiO ₂ (wt.%)	56.90	57.30	58.10	56.60	56.50	55.90	57.00	55.80	63.90	62.10	63.40	63.20
TiO ₂	0.41	0.36	0.41	0.50	0.73	0.72	0.51	0.59	0.56	0.62	0.08	0.04
Al ₂ O ₃	18.70	19.20	18.20	18.50	18.50	18.60	18.30	18.80	19.40	18.90	19.70	20.30
MnO	0.16	0.28	0.00	0.00	0.23	0.00	0.18	0.31	0.27	0.37	0.15	0.14
MgO	1.42	1.30	1.32	1.60	1.53	1.77	1.79	1.70	0.00	0.29	0.12	0.10
Fe ₂ O _{3T}	5.45	5.29	5.15	5.81	5.48	6.34	6.01	6.42	1.18	2.86	0.77	0.06
CaO	4.35	4.24	3.91	4.89	4.86	4.78	4.83	4.81	1.83	1.29	2.15	1.86
Na ₂ O	3.11	3.07	3.39	3.18	2.92	3.35	2.87	3.02	7.23	6.51	7.18	7.11
K ₂ O	9.37	8.80	9.28	8.61	8.88	8.19	8.06	8.17	5.51	6.82	6.46	7.02
P ₂ O ₅	0.15	0.17	0.25	0.37	0.38	0.43	0.43	0.41	0.09	0.19	0.00	0.18
sum	100	100	100	100	100	100	100	100	100	100	100	100
Mortars	A63M <i>glass</i>	A63M <i>glass</i>	A63M <i>glass</i>	A63M <i>glass</i>	A63M <i>glass</i>	A63M <i>glass</i>	A63M <i>glass</i>	A63M <i>glass</i>	A63M <i>glass</i>	A63M <i>glass</i>	A63M <i>glass</i>	A63M <i>glass</i>
SiO ₂ (wt.%)	61.00	60.80	60.30	60.70	59.60	61.00	61.30	62.40	61.20	61.00	61.90	
TiO ₂	0.76	0.53	0.80	0.52	0.42	0.21	0.24	0.58	0.77	0.99	0.43	
Al ₂ O ₃	18.50	18.40	17.90	18.10	18.30	18.30	18.10	17.80	18.20	18.90	18.40	
MnO	3.90	3.39	3.79	3.58	4.22	3.69	3.06	3.33	3.07	2.41	2.97	
MgO	0.11	0.28	0.11	0.16	0.59	0.00	0.25	0.07	0.30	0.00	0.22	
Fe ₂ O _{3T}	0.46	0.75	0.59	0.60	0.84	0.36	0.61	0.18	0.31	0.52	0.63	
CaO	2.29	2.58	2.73	2.61	2.45	2.42	2.63	1.68	2.16	2.43	1.75	
Na ₂ O	4.63	4.81	5.17	4.91	3.17	4.82	4.93	5.68	5.59	4.23	4.83	
K ₂ O	8.17	8.09	8.50	8.56	10.02	9.17	8.65	8.21	8.35	9.26	8.64	
P ₂ O ₅	0.22	0.36	0.06	0.28	0.33	0.00	0.20	0.00	0.00	0.28	0.19	
sum	100	100	100	100	100	100	100	100	100	100	100	
Cocchiopesto	A63C <i>glass</i>	A63C <i>glass</i>	A63C <i>glass</i>	A63C <i>glass</i>	A63C <i>glass</i>	A63C <i>glass</i>	A63C <i>glass</i>	A63C <i>glass</i>	A63C <i>glass</i>	A63C2 <i>glass</i>	A63C2 <i>glass</i>	A63C2 <i>glass</i>
SiO ₂ (wt.%)	60.4	60.3	61.4	61.1	60.9	61.9	61.1	62.2	60.23	62.81	63.10	
TiO ₂	0.49	0.47	0.18	0.43	0.23	0.26	0.06	0.06	0.19	0.36	0.45	
Al ₂ O ₃	19.2	18.9	18.6	18.6	18.3	18.4	18.3	18.5	18.46	17.69	18.36	
MnO	3.44	3.15	3.33	3.23	3.58	2.96	3.65	2.90	3.68	3.27	2.89	
MgO	0.04	0.26	0.00	0.05	0.15	0.39	0.00	0.15	0.41	0.24	0.08	
Fe ₂ O _{3T}	0.47	0.47	0.43	0.27	0.51	0.54	0.45	0.48	0.77	0.32	0.17	
CaO	2.30	2.45	2.25	2.28	2.47	2.32	2.47	2.07	2.96	2.07	1.91	
Na ₂ O	4.31	4.47	4.69	4.48	4.38	4.60	4.49	4.44	3.31	5.30	4.25	
K ₂ O	9.37	9.61	8.88	9.42	9.35	8.69	9.26	9.19	9.72	7.91	8.69	
P ₂ O ₅	0.00	0.00	0.28	0.12	0.18	0.00	0.20	0.00	0.28	0.03	0.11	
sum	100	100	100	100	100	100	100	100	100	100	100	

A63GT sample, glassy shard fragments are often altered in alkali feldspar, and show slightly higher SiO_2 (62.3-64 wt.%) and $\text{Na}_2\text{O}+\text{K}_2\text{O}$ (12.8-13.9 wt.%) values than A63YT and A63YTT samples. Glasses

from A63M, A63C and A63C2 samples, show a quite similar chemical composition. SiO_2 vary between 59.6 and 63.1 wt.% and $\text{Na}_2\text{O}+\text{K}_2\text{O}$ between 12.8 and 14.0 wt.%.

Table 2. Zeolites and alkali feldspar analyses from tuffs samples.

	A63YT <i>phillipsite</i>	A63YT <i>chabazite</i>	A63YTT <i>chabazite</i>	A63GT <i>alkali feldspar</i>
SiO_2 (wt.%)	54.70	46.30	36.40	63.70
TiO_2	0.00	0.21	0.25	0.17
Al_2O_3	18.50	15.40	11.50	18.40
MnO	0.00	0.00	0.24	0.00
MgO	0.03	0.10	0.04	0.08
FeO	0.09	0.27	0.00	0.31
CaO	3.79	7.04	4.85	0.63
Na_2O	1.41	0.48	0.15	3.88
K_2O	8.78	6.63	9.06	10.79
P_2O_5	0.15	0.00	0.00	0.00
BaO	0.34	0.00	0.17	0.00
SO_3	0.00	0.17	0.00	0.14
Cl-	0.07	0.00	0.13	0.00
sum	87.9	76.6	62.8	98.1

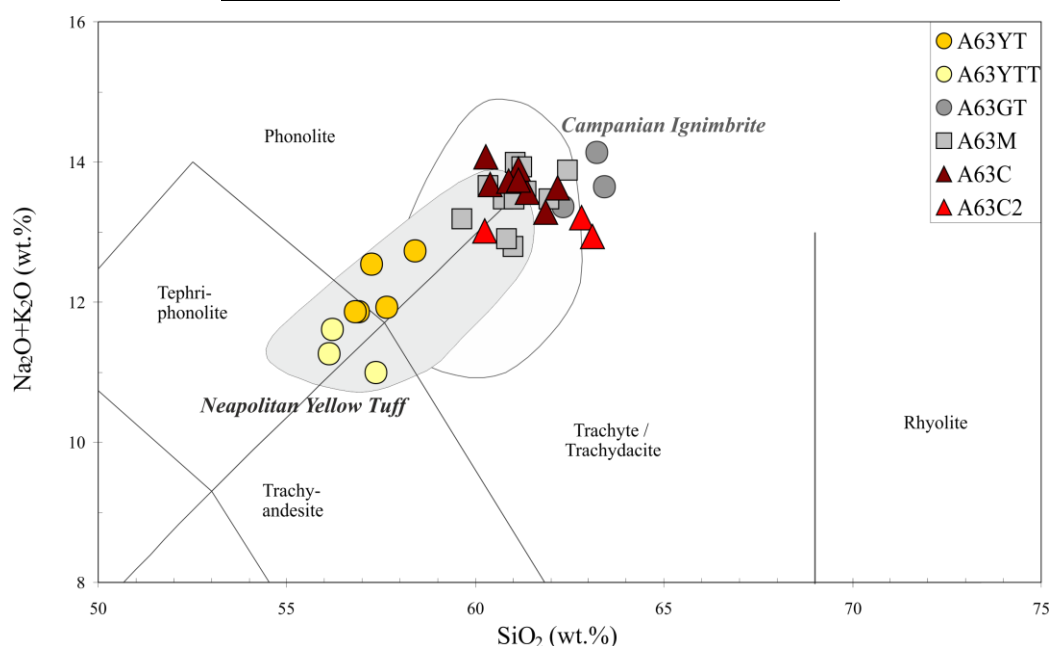


Figure 12. TAS diagram (Le Bas *et al.*, 1986) glasses (juvenile materials). Neapolitan Yellow Tuff and Campanian Ignimbrite fields are from Rosi and Sbrana (1987), Scarpati *et al.* (1993), Orsi *et al.* (1996), Signorelli *et al.* (1999), Melluso *et al.* (1995), Civetta *et al.* (1997), Pappalardo *et al.* (2002) and Fedele *et al.* (2008).

Mineralogical analysis (XRPD)

Mineralogical compositions are reported in Table 3.

Yellow tuffs samples, A63YT and A63YTT, show very similar mineralogical composition. They are both characterized by the presence of sanidine, phillipsite, chabazite, mica, pyroxene and subordinate calcite. The grey tuff sample (A63GT) shows the presence of sanidine, plagioclase, sodalite, amphibole, clinopyroxene, mica and magnetite.

The XRD pattern, of A63M mortar, highlights the presence of feldspar, calcite, phillipsite, chabazite, clinopyroxene and mica.

Two *cocciopesto* (A63C and A63C2) samples show the presence of calcite, sanidine and mica.

Two carbonatic samples, A63L and A63MA, macroscopically classified as micritic limestone and a white marble, used as building stone and as architectural element are composed by dominant calcite.

Table 3. Mineralogical composition.

	Sanidine	Plagioclase	Phillipsite	Chabazite	Mica	Clinopyroxene	Calcite	Others
A63YT	x		x	x	x	x	x	
A63YTT	x		x	x	x	x	x	
A63GT	x	x			x	x	x	Am, Sdl, Mag
A63M	x		x	x	x	x	x	
A63C	x				x	x	x	
A63C2	x				x	x	x	
A63L							x	
A63MA							x	

Am= Amphibole, Sdl= Sodalite, Mag= Magnetite

6. DISCUSSION

Data obtained from mineralogical petrographic and microchemical analyses allowed us to draw some hypothesis on the provenance of building materials.

Tuffs

Mineralogical investigation performed on A63YT and A63YTT samples, showed the presence of phillipsite and chabazite, the typical zeolites of Phlegraean tuffs.

The comparison between XRPD patterns of A63YT and A63YTT samples with typical pattern of a Neapolitan Yellow Tuff (Colella et al., 2017) suggests the strong similarity between analysed samples and Neapolitan Yellow Tuff (NYT) formation.

Subordinate calcite, evidenced by XRPD, is probably due to the contact between bedding mortars and tuff blocks.

A63GT sample was compared with a typical XRPD pattern from Campanian Ignimbrite (CI) grey facies. Also in this case, the two samples are quite compa-

table and allowed to ascribe the investigated material to the upper portion of the CI formation, and, more precisely, its most widespread facies, WGI (Welded Grey Ignimbrite) (Langella et al., 2013).

The above assertions were also confirmed by the results of microchemical analyses (EDS) performed on juvenile fraction of A63YT, A63YTT and A63GT samples. TAS diagram confirms that data points obtained from A63GT sample are within the area of the Campanian Ignimbrite rocks, while those from A63YT and A63YTT samples fall within the Neapolitan Yellow Tuff field, even though some points are close to Campanian Ignimbrite area (namely Lithified Yellow Tuff facies - LYT) (Fig. 12).

Combining information from outcrops of the main Campanian tuffs (Langella et al., 2013; Colella et al., 2017) with the ancient Roman road maps (De Bonis et al., 2013 and references therein) it is reasonable to hypothesize that yellow tuffs have a local provenance, close to archaeological site, while grey tuff sample comes from the northern sector of the Campania region (Fig. 13).



Figure 13. Sketch map of Campanian Ignimbrite outcrops (modified after Langella et al., 2013). LYT= Lithified Yellow Tuff - Yellow facies; WGI= Welded Grey Ignimbrite - Grey facies.

Technology and provenance of mortars

Mortar and *cocciopesto*, despite differences in texture, show quite similar raw materials. Those can be basically referred to limestones (lime-based binder and carbonatic fragments) along with volcanic aggregates (pumice and loose crystals). Mineralogical composition and EDS analyses confirmed the use of Phlegraean materials also for aggregates.

Mortar preparation, mixing lime with pozzolana, highlights the awareness of ancient workers of the physical and technical properties of these geomaterials (Belfiore *et al.*, 2015; Miriello *et al.*, 2010; Izzo *et al.*, 2016). As regards *cocciopesto*, the use of ceramic fragments along with volcanic aggregates represents another technological skill used during Roman age to provide a reddish color and a better hydraulicity to mortars (Fig. 8c). Such high hydraulicity (evidenced by reaction rims of ceramic fragments) is the result of an accurate selection, preparation and mixing of raw geomaterials, supplied by the geological availability in the area surrounding the archaeological site.

Limestones and marble

As regards carbonatic geomaterials (limestones and marbles) no specific indication could be assessed, but it is reasonable to think that, through *Via Domitiana*, such materials may have reached Cuma

from the north and, in the case of marble, may come from recycling from other buildings.

7. CONCLUSIONS

This research, carried out on the “*Complesso monumentale della Sfinge*”, evidenced the wide use, as building stone, of geomaterials (natural and artificial) closely related to the geology of the area. Wide distribution of volcanic tuffs along with their easy workability and good petrophysical features favoured the use, since Roman age, of Phlegraean Tuffs (de Gennaro *et al.*, 2013). The whole complex was built with Neapolitan Yellow Tuff; this material was preferred in the following three building phases. A grey tuff with decorative functions was used too. This material can be ascribed to the grey facies (Welded Grey Ignimbrite) of Campanian Ignimbrite formation. As regards artificial geomaterials, such as mortars and *cocciopesto*, the use of volcanic aggregates of Phlegraean origin was also privileged. The mix design is the results of a mixture of lime and pozzolanic aggregates. Although there is no specific information, we can identify only two non-local materials: micritic limestones and statuary marble. The first one constitutes ten *cippi* of the fence (structural function) while the second one was used for prestigious coating elements (decorative function).

ACKNOWLEDGEMENTS

Authors wish to thank Dr. Roberto de Gennaro and Dr. Sergio Bravi for SEM-EDS and for thin sections preparation, respectively. This research was granted by PON “SINAPSIS” (Sistema Protezione Siti Sensibili – PON01_01063) national research project.

REFERENCES

- Belfiore, C.M., Fichera, G.V., La Russa, M.F., Barca, D., Galli, G., Ruffolo, S.A. and Pezzino, A. (2015) A multidisciplinary approach for the archaeometric study of pozzolanic aggregate in Roman mortars: the case of villa dei quintili Rome, Italy. *Archaeometry*, Vol. 57, pp. 269–296.
- Brun J. P., Munzi P. and Botte, E. (2017) Cuma il monumento funerario della Sfinge (A63) nella necropoli della Porta Mediana. Complessi monumentali e arredo scultoreo nella Regio I Latium et Campania. *Nuove scoperte e proposte di lettura in contesto. Atti del Convegno internazionale, Napoli 5 e 6 Dicembre 2013 (a cura di Capaldi C. e Gasparri C.)*, Naus Editoria, pp. 137–164.
- Civetta, L., Orsi, G., Pappalardo, L., Fisher, R.V., Heiken, G. and Ort, M. (1997) Geochemical zoning, mingling, eruptive dynamics and depositional processes – the Campanian Ignimbrite, Campi Flegrei caldera, Italy. *Journal of Volcanology and Geothermal Research*, Vol. 75, pp. 183–219.
- Colella, A., Di Benedetto, C., Calcaterra, D., Cappelletti, P., D’Amore, M., Di Martire, D., Graziano, S.F., Papa, L., de Gennaro, M. and Langella, A. (2017) The Neapolitan Yellow Tuff: An outstanding example of heterogeneity. *Construction and Building Materials*, Vol. 136, pp. 361–373.
- Conticelli, S., Melluso, L., Perini, G., Avanzinelli, R. and Boari, E. (2004) Petrologic, geochemical and isotopic characteristics of potassic and ultrapotassic magmatism in central-southern Italy: inferences on its genesis and on the nature of mantle sources. *Periodico di Mineralogia*, Vol. 73, pp. 135–164.
- De Bonis, A., Grifa, C., Cultrone, G., De Vita, P., Langella, A. and Morra, V. (2013) Raw Materials for Archaeological Pottery from the Campania Region of Italy: a petrophysical characterization. *Geoarchaeology*, Vol. 28, pp. 478–503.

- De Bonis, A., Febraro, S., Germinario, C., Giampaola, D., Grifa, C., Guarino, V., Langella, A. and Morra, V. (2016) Distinctive volcanic material for the production of Campana A ware: The workshop area of Neapolis at the Duomo Metro Station (Naples, Italy). *Geoarchaeology*, Vol. 31(6), pp. 437-466.
- de Gennaro, M., Calcaterra, D. and Langella, A. (Eds) (2013) *Le pietre storiche della Campania: dall'oblio alla riscoperta*. Luciano Editore, Napoli, pp. 155-178.
- De Luca, R., Miriello, D., Pecci, A., Dominguez-Bella, S., Bernal-Casasola, D., Cottica, D., Bloise, A. and Crisci, G.M. (2015) Archaeometric study of mortars from the Garum Shop at Pompeii, Campania, Italy. *Geoarchaeology*, Vol. 30, pp. 330-351.
- Deino, A. L., Orsi, G., De Vita, S. and Piochi, M. (2004) The age of the Neapolitan Yellow Tuff caldera-forming eruption (Campi Flegrei caldera - Italy) assessed by ⁴⁰Ar/³⁹Ar dating method. *Journal of Volcanology and Geothermal Research*, Vol. 133, pp. 157-170.
- Fedele, L., Scarpati, C., Lanphere, M., Melluso, L., Morra, V., Perrotta, A., Ricci, G. (2008) The Breccia Museo formation, Campi Flegrei, southern Italy: geochronology, chemostratigraphy and relationship with the Campanian Ignimbrite eruption. *Bulletin of Volcanology*, Vol. 70, pp. 1189-1219.
- Guarino, V., Wu, F.Y., Melluso, L., Gomes, C.B., Tassinari, C.C.G., Ruberti, E. and Brilli, M. (2017) U-Pb ages, geochemistry, C-O-Nd-Sr-Hf isotopes and petrogenesis of the Catalão II carbonatitic complex (Alto Paranaíba Igneous Province, Brazil): implications for regional-scale heterogeneities in the Brazilian carbonatite associations. *International Journal of Earth Sciences (Geol Rundsch)*, Vol. 106(6), pp. 1963-1989.
- Izzo, F., Arizzi, A., Cappelletti, P., Cultrone, G., De Bonis, A., Germinario, C., Graziano, S.F., Grifa, C., Guarino, V., Mercurio, M., Morra, V. and Langella, A. (2016) The art of building in Roman Period (89 B.C.-79 A.D.): Mortars, plasters and mosaic floors from Ancient Stabiae (Naples, Italy). *Construction & Building Materials*, Vol. 117, pp. 129-143.
- Langella, A., Bish, D.L., Cappelletti, P., Cerri, G., Colella, A., de Gennaro, R., Graziano, S.F., Perrotta, A., Scarpati, C. and de Gennaro, M. (2013) New insights into the mineralogical facies distribution of Campanian Ignimbrite, a relevant Italian industrial material. *Applied Clay Science*, Vol., 72, pp. 55-73.
- Le Bas, M.J., Le Maitre, R.W., Streckeisen, A. and Zanettin, P. (1986) A chemical classification of volcanic rocks based on the Total Alkali-Silica diagram. *Journal of Petrology*, Vol. 27, pp. 745-750.
- Mahmoud, H.M, Kantiranis, N and Stratis, J (2012) A technical characterization of Roman plasters, Luxor Temple, Upper Egypt. *Mediterranean Archaeology and Archaeometry*, Vol. 12, No 2, pp.81-93.
- Melluso, L., de Gennaro, R., Fedele, L., Franciosi, L. and Morra V. (2012) Evidence of crystallization in residual, Cl-F-rich, agpaitic, trachyphonolitic magmas and primitive Mg-rich basalt-trachyphonolite interaction, in the lava domes of the Phlegrean Fields (Italy). *Geological Magazine*, Vol., 149, pp. 532-550.
- Melluso, L., Guarino, V., Lustrino, M., Morra, V. and de Gennaro, R. (2017) The REE- and HFSE-bearing phases in the Itatiaia alkaline complex (Brazil), and geochemical evolution of feldspar-rich felsic melts. *Mineralogical Magazine*, Vol. 81(2), pp. 217-250..
- Melluso, L., Morra, V., Perrotta, A., Scarpati, C. and Adabbo, M. (1995) The eruption of the Breccia Museo (Campi Flegrei, Italy): fractional crystallization processes in a shallow, zoned magma chamber and implications for the eruptive dynamics. *Journal of Volcanology and Geothermal Research*, Vol. 68, pp. 325-339.
- Miriello, D., Barca, D., Bloise, A., Ciarallo, A., Crisci, G.M., De Rose, T., Gattuso, C., Gazineo, F. and La Russa, M.F. (2010) Characterisation of archaeological mortars from Pompeii (Campania, Italy) and identification of construction phases by compositional data analysis. *J. Archaeol. Sci.* 37 2207-2223.
- Morra V., Calcaterra D., Cappelletti P., Colella A., Fedele L., de' Gennaro R., Langella A., Mercurio M., de' Gennaro M., Urban geology: Relationships between geological setting and architectural heritage of the Neapolitan area, in: M. Beltrando, A. Peccerillo, M. Mattei, S. Conticelli, C. Doglioni (Eds.), *The geology of Italy: Tectonics and life along plate margins*, Journal of the Virtual Explorer, vol. 36, 2010, pp. 1-59.
- Pappalardo, L., Civetta, L., de Vita, S., Di Vito, M., Orsi, G., Carandente, A. and Fisher, R.V. (2002) Timing of magma extraction during the Campanian Ignimbrite eruption (Campi Flegrei Caldera). *Journal of Volcanology and Geothermal Research*, Vol. 114, pp. 479-497.
- Perrotta, A., Scarpati, C., Luongo, G. and Morra, V. (2006) The Campi Flegrei caldera boundary in the city of Naples. In *Volcanism in the Campania Plain: Vesuvius, Campi Flegrei and Ignimbrites*. (ed. B. De Vivo), *Developments in Volcanology no. 9*. Amsterdam, Elsevier, pp. 85-96.

- Orsi, G., de Vita, S. and Di Vito, M. (1996) The restless, resurgent Campi Flegrei nested caldera (Italy): constraints on its evolution and configuration. *Journal of Volcanology and Geothermal Research*, Vol. 74, pp. 179–214.
- Rosi, M. and Sbrana, A. (1987) The Phlegraean Fields. *C.N.R. Quaderni de "La ricerca scientifica"*, Vol., 114, pp 1-175.
- Scarpati, C., Cole, P. and Perrotta, A. (1993) The Neapolitan Yellow Tuff - a large volume multiphase eruption from Campi Flegrei, Southern Italy. *Bulletin of Volcanology*, Vol. 55, pp. 343–356.
- Signorelli, S., Vaggelli, G., Francalanci, L. and Rosi, M. (1999) Origin of magmas feeding the Plinian phase of the Campanian Ignimbrite eruption, Phlegrean Fields (Italy): constraints based on matrix-glass and glass inclusion compositions. *Journal of Volcanology and Geothermal Research*, Vol. 91, pp. 199–220.